Proceedings of the 7th International Symposium on Cavitation
CAV2009
August 17-22, 2009, Ann Arbor, Michigan, USA

CAV2009 – Paper No. 180

ON SOME PHYSICS TO CONSIDER IN NUMERICAL SIMULATION OF EROSIVE CAVITATION

Göran Bark
Chalmers University of Technology
Göteborg, Sweden

Mikael Grekula
SSPA Sweden AB
Göteborg, Sweden

Rickard E Bensow
Chalmers University of Technology
Göteborg, Sweden

Nabila Berchiche
Chalmers University of Technology
Göteborg, Sweden

ABSTRACT

This paper discusses several mechanisms in erosive cavitation, which are all important to capture, and study, when assessing the risk of erosion. In particular we introduce the concept of primary and secondary cavitation in order to put emphasis on a particular class of mechanisms: cavitation created in the secondary flow field governed by, e.g., a shedding or collapse of a primary created cavity. These secondary cavities are almost always erosive and have previously not been much described in the literature. The role of cloud cavitation is partly reconsidered and a hypothesis for development of vortex group cavitation, a type of secondary cavitation, is presented. An underlying part of the discussion is how the described cavitation mechanisms influence numerical simulation of cavitation nuisance.

INTRODUCTION

The details of the erosion process can differ depending on hydrodynamic conditions and solid body material. In general terms, however, cavitation erosion on hydraulic equipment, as e.g. propellers, can be said to be the result of repeated and very local stresses, spreading into the solid matter, due to cavity collapses occurring on, or very close to the body surface.

Already from this simple view follows that prediction of cavitation erosion requires at least a quantitative determination of hydrodynamic force amplitudes, including the distribution in space and time, and the corresponding response of the solid body to this load. Considering the long exposure times that typically occur, even an influence of the chemical properties of the liquid and solid cannot always be excluded. The problem is complex and in engineering applications partly empirical methods have been a necessary approach. An overview of the physics in general, hydrodynamics, scaling principles, related prediction methods and relevant data are given by Lecoffre (1999), chapter 11, and by Franc and Michel (2004), chapter 12. An example of a more extended review of the research is presented by Franc (1997).

The wide span of hydrodynamic conditions and cavity configurations at which propeller erosion typically occurs, and the fact that a set of well proven hydrodynamic solutions on hull and propeller often is applied, has resulted in a certain focus on visual assessment of cavitation aggressiveness. Preferably is however a visual assessment supplemented by at least application of a soft paint as erosion sensor. This seemingly primitive technique has however, particularly when a soft paint is used as sensor, been demonstrated to be surprisingly reliable, despite the extremely simplified scaling of the solid material.

A reason for the success is that in propeller cavitation certain processes control most of the significant erosion cases - and that these processes usually can be well captured at model tests in cavitation tunnels. The understanding of the particular flow and cavitation, and how it can be modified by design, is the daily discussion in testing laboratories with a typical project flow of one case per week, during which a simple standard erosion study may be finished within a half day, including the analysis. With the aim to tailor the flow and numerical simulation of cavitation dynamics, a visual analysis is a central part of the work, and is then an obvious tool in such work.

Extended principles for analysing the erosion risk by a study of the cavity kinematics only, still however preferably supported by a paint test and recording collapse pulses, are described in the EROCAV observation handbook, Bark *et al.* (2004). These guidelines were primarily written for an experimental procedure but with the progress of numerical

simulations of cavity dynamics in mind. Although measurement of collapse pulses in principle is relevant for erosion assessment, the measurement as well as interpretation of the data is often difficult to achieve in a propeller test. Uncertainty follows e.g. because the balance between simple collapse pulses generated close to the body surface and microjet impacts on the body surface are not possible to discriminate and hence pulses from different processes may be compared.

Considering this background and approach in propeller design, a main research task is the understanding of the large to medium-scale hydrodynamics of cavitation. With the progress in cavitation CFD towards capturing most observable dynamics, this becomes even more important. A process, that simply is present through the physics in a model test, may still require certain awareness at simulation.

A previous step in this task was made in the EROCAV project, Bark *et al.* (2004). There, e.g. the group of cavitating vortices here called "vortex group cavitation" downstream a sheet cavity was identified as erosive, sometimes significantly and sometimes only slightly or not at all, despite being nasty looking. A first inspection of high-speed films of moderate frame rate, 5000 - 8000 fps, would suggest that the cavitating vortices were rebounded after fast collapses not resolved by the applied frame rate. This interpretation was however not entirely convincing and it was early planned to make a supplementary study. The plan was further enhanced when the simulations (Huuva 2007, 2008, Bensow 2008) of the Delft Twist 11 foil indicated a complex vortex development that, despite the analysis made by Foeth (2008), was still not fully understood.

The content of the present paper is however wider with discussion of cavitation mechanisms and physics in general, that have to be considered in numerical simulations of cavitation dynamics leading to erosion. We limit the discussion by disregarding the response of the solid material, an approach corresponding to a cavitation experiment aimed for visual assessment, possibly including collapse pulse recordings, but without the soft paint or metal as erosion sensor. The corresponding simulations of the hydrodynamics need to be in the high-end region; a more precise discussion on what this means is delayed until the conclusions. The actual erosion risk assessment will not be much addressed here; it is assumed to be made according to the EROCAV observation handbook.

The structure of the paper is as follows: We will start by describing some general properties of erosive cavitation, focusing on understanding of the different routes of cascading energy, from large to medium small scales into erosive collapses. Then the terminology of primary and secondary cavitation is introduced in order to put focus on and discuss certain aspects of the mechanisms that can easily be overlooked; this discussion will be supplemented by comments on collapse symmetry and the erosiveness of cloud cavitation. Finally, we summarize the results in the concluding section and comment on how these results relate to current efforts on numerical simulation of cavitation dynamics.

SOME CHARACTERISTICS OF EROSIVE CAVITATION

Cavitation scales and erosion

A number of studies support the idea that the development of the final part of the collapse of a cavity is directly related to the contribution to cavitation erosion from a single collapse. The late development controls the final concentration, here referred to as focusing, and transfer of collapse energy to the solid material. The mechanics of the energy transfer are, according to generally accepted observations, assumed to consist of microjet impacts on the body surface or generation of pressure pulses by a collapse very close to the body surface, or a combination of both. Both alternatives are much influenced by the symmetry properties of the collapse dynamics.

At sampling the cavity collapse it is found that the minimum size of the cavity in practice occurs between the smallest recorded collapsing cavity and the smallest recorded rebounding cavity. The minimum size and kinematical data around the minimum point are thus only approximately known. The problem is made difficult by the small size and accelerating motion during the late part of the collapse. To trace the cavity as precise as possible close to its minimum size is however assumed to improve the erosion assessment, because the aggressiveness of the collapse can, for a given initial size, be assumed to increase as the minimum size decreases.

Although some general data for near final collapse velocities related to erosion are indicated by Lecoffre (1999) they are not easily applicable for formulation of erosion criteria at observable scales for the different collapse configurations that occurs in e.g. propeller flow. It is supposed however that also in the lack of such quantitative criteria it can be useful to make relative comparisons of near final collapse velocity, acceleration or pressure amplitude. In the case of medium or significant erosion due to typical propeller cavitation it is e.g. usually possible to identify a risk of erosion by observation of the collapse by high-speed video. This assessment is mainly based on the near final behaviour of the collapse, particularly on the possible existence of a rebound, (Bark et al. 2004). Similar ideas can also be extracted from Lecoffre (1999) and Franc and Michel (2004). To roughly estimate the near maximum collapse velocity, occurring just before the start of the retardation initiating the rebound and generation of the maximum collapse pulse, typically requires a frame rate of at least 100 000 frames/s at typical model test conditions. Due to the small size of the cavity when this occurs, also very high spatial resolution is required. Still, a trained observer can sometimes assess a collapse as erosive or not already at 5000 frames/s, or even by an observation in stroboscopic light.

Observations covering the final collapse and rebound are doubtless key information for erosion assessment, but due to the resolution requirements the observations are difficult to make – and they do not alone bring all wanted information. Although final collapse data, as pulse amplitude, are uniquely determined by the initial conditions, geometrical configuration and pressure/flow history there are many possible conditions generating this amplitude in the same point. For design considerations it is almost equally important to understand why and how an erosive collapse develops from an early state, as it is to detect the event, and hence the entire development towards

the collapse has to be recorded. This is a main idea applied in also the EROCAV handbook, where it is even argued that useful information may still be gained even if tracing of the collapse is stopped well before the final collapse, particularly if a rebound is recorded. However, the analysis usually gains by tracing a collapse as close as possible towards the final point.

As indicated the collapse energy finally focused reflects the initial conditions and collapse forcing pressure throughout the collapse. When a cavity disintegrates or the collapse is temporarily interrupted, due to the pressure history, we have to notice the time at which the focusing starts of the energy that effectively contributes to erosion, as further discussed by Grekula et al. (2009). Typically, only a small part of the total potential energy initially related to even a rather coherently collapsing cavity may finally be converted into erosion work. The disintegration of a cavity occurs e.g. due to re-entrant jet flow and is typically a large or medium scale process. The initial conditions and collapse forcing pressure history as well are related to the global flow controlled by design, and can mainly be analysed by well resolved CFD.

A critical issue, related to identification of the initial conditions for an erosive collapse, is to know the minimum value of a quantity, e.g. the initial cavity volume that may result in erosion. This issue may result in scale and approximation errors, particularly at weak erosion. It is e.g. convincingly confirmed by full scale correlations that erosion generated by large and medium scale cavities often is well captured by a paint test in a cavitation tunnel, an assessment that also can be expected from a visual analysis of the cavity by high speed video. It is more difficult to confirm the ability of a model test to predict, by paint test, visual and/or acoustical analysis, the erosion by small moderately fast collapsing cavities that at full scale are only weakly erosive. The possible scale effect includes the possibility that the small cavity does not even occur at the model test. Most likely will similar situations, due to approximations in model or grid, occur at numerical simulations.

A conclusion *from this discussion is thus that recording and analysis have to be done of a range of scales, from the largest to the smallest recordable scale, throughout which the accelerating collapse is focusing the energy that controls generation of the erosion. Tracing this focusing process backwards to its initial condition is a key step towards understanding design selections.* The ideal is if the collapse can be followed through the rebound and the maximum of the collapse pulse. The pulse amplitude may be useful for relative comparisons but is usually unreliable as absolute data, the reason being its dependence on the cavity content, which is mainly unknown, both the behaviour and the quantity. Useful engineering conclusions can however be made before the generation of the final collapse pulse occurs. Based on empirical support we assume in this discussion that an increase of collapse pulse amplitude correlates with increased erosiveness, neglecting a possible change of a different balance between erosion by microjet impacts and by collapses at a distance from the body surface. Possible microjets, not resolved in present CFD or experimental recordings, are e.g. assumed to be forced, and thus enhanced, by the collapse pulse.

Ways towards erosive cavitation

We identify now the basic ways along which a cavity may develop towards an erosive collapse, and that have to be captured in a simulation.

A necessary condition for development of an erosive collapse is the formation of a transient cavity, i.e. a cavity that after the growth, performs a fast collapse. By the expansion of the cavity, a potential energy is created in the surrounding liquid, proportional to the cavity volume and the surrounding pressure. During the collapse this energy is transferred to kinetic energy. By kinematical focusing of the kinetic collapse energy, a part is transferred to the solid material as "erosion work," highly concentrated in space and time by the hydrodynamic and acoustical focusing process.

Because the present analysis of erosion risk is mainly based only on kinematical focusing of collapse energy related to a single cavity, usually without even knowing the collapse pulse(s), and with no material response included, the controlling quantity is assumed to be the collapse *energy*. For material response the duration of the energy transfer is typically important, as is the amplitude distribution during the energy transfer, and a *power*, defined by a properly selected time interval, would be a more adequate quantity.

We identify the following developments as the typical main ways by which focusing and erosive cavities are formed:

1. *Direct creation of a travelling cavity*, i.e. creation of a cavity the upstream edge of which is not fixed to a stationary starting/detachment point; the basic example is a single travelling cavitation bubble.
2. *Shedding of a part of an attached cavity*. The shedding can develop due to different processes, but typically the process is controlled by internal jets, i.e. re-entrant or side-entrant jets.
3. *The upstream desinence of an initially attached cavity***,** e.g. a sheet disappearing from the leading edge due to a decreasing angle of attack. This could also be considered both as a special case of 1 above, a delayed creation of a travelling cavity, or a limiting version of case 2.
4. *The upstream moving collapse of an attached cavity***.** The basic example is the partly glassy sheet attached to an upstream position during its entire life. This primary collapse may result in erosion, but more often new erosive cavitation is generated as the trailing edge of the primary cavity moves upstream during the collapse.
5. *Creation of secondary cavities*. This is a particular class of transient cavitation, whose erosiveness can vary from non-erosive to severe. This is a main new concept introduced in the next section.

Depending on the particular aim, different approximations can be done at selection of the main numerical approach, regarding e.g. viscosity, compressibility, vaporization models, permanent gas, but common is that without a very high resolution, in time as well as space, the simulation will not capture all potentially important effects. Nevertheless, approximate simulations neglecting e.g. secondary cavitation may still be useful supplements to model testing etc. for early design analysis.

CONCEPT OF PRIMARY AND SECONDARY CAVITIES

The cavitation process is composed of a number of mechanisms that gradually may vary in importance as the cavitation develops. At model testing the hope is that all mechanisms occurs to the same amount as they do at full scale. If this is not the case the model test suffers from scale effects. At numerical simulation approximations may have similar effects. From engineering points of view it can be important to understand how the effects influence a prediction, e.g. if a certain erosive cavitation is suppressed by scale or approximation effects. A decomposition of the cavitation process into parts, e.g. dominated by different parts of the physics, can be useful for understanding the origin of scale and approximation effects, and the possibility to reduce them. For numerical simulation a decomposition of the cavitation process can indicate requirements on resolution and consideration of certain physics, as compressibility or viscosity.

Based on experimental data and motivated by physics and engineering aspects we introduce here particularly the concept of secondary cavities. The experimental work that formed the basis for this concept is briefly described in the appendix. Experiments were made with foils and propellers and include generic processes valid for a number of applications.

Definition of primary and secondary cavity

With the idea to capture and put focus on particular cavitation processes relevant for erosion assessment, and that require special attention at modelling. We suggest the definition:

Definition:

*By a **primary cavity** we mean a cavity developing in a flow and pressure field which is primarily controlled by inflow and geometrical properties of the domain. An example of a primary cavity is the original development of a sheet.*

*By a **secondary cavity** we mean a cavity that, except for a marginal initial volume that may originate from the primary vapour volume, develops as an effectively new cavity, the development of which is controlled by the flow and pressure fields induced by the primary cavity, particularly the collapse motion, in combination with the global flow field. See Figure 1.*

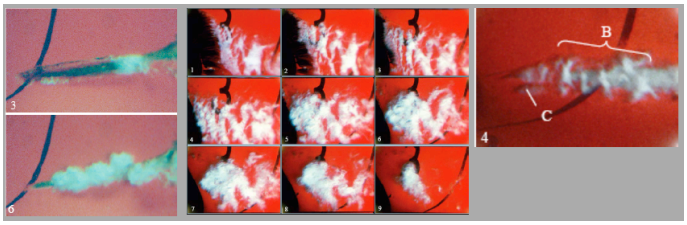

Figure 1 *Examples of primary and secondary cavities on the propeller P1477. The two frames to the left: Upper; primary cavity during collapse, Lover; secondary cavity (rebound, cloudy); Middle: Development of secondary cloud cavitation (vortex group cavitation) downstream the primary sheet seen far left in the upper row; Right: Secondary cavitation (vortex group cavitation).*

The definition is unsharp in the sense that there is typically a gradual transition, from a pure redistribution, by action of e.g. a re-entrant jet, of the vapour volume of the primary cavity into a reshaped primary cavity - to the creation of totally new vapour volume, i.e. a pure secondary cavity, created by excitation of cavitation nuclei that at least for some time have been compressed to "nuclei size". Examples of secondary cavities are rebounds controlled by elastic compression, certain cavities created by shear, vortices or other fields induced by the primary cavity. Examples of a rebound and shedding vortex group cavitation are shown in Figure 1.

The definition could alternatively be interpreted to define e.g. any part shed from the primary cavity as a secondary cavity. This would be more straight but would also detract the intended focus on certain processes requiring special attention at simulation, and thus we preliminary avoid to consider vapour volumes shed from the primary cavity by a simple processes as local cavitation desinence or simple cut off by re-entrant jets as secondary cavitation. Applying the wider, alternative, interpretation of the definition is however free of choice and does not change the idea to identify a class of cavities created as a result of the dynamics of the original cavity.

Basically, there is no special difference between primary and secondary cavities - the development of secondary cavitation is a direct continuation of the process started by the development of the primary cavity, but different sub processes controlled by shear, compressibility etc. may be differently important during the primary and secondary phases.

To demonstrate the intention with the definition the shedding due to a re-entrant jet is considered. The shedding of a void from a sheet is in a sense completed already when a durable and tight liquid-liquid contact between the re-entrant jet and the external flow is established. After some time the void isolated from the original cavity by the re-entrant jet is cut-off and transported downstream. None of these two voids are here interpreted as secondary cavities. According to Mørch *et al.* (2003) creation of cloud cavitation in this case is first initiated by surface tension, directly when the jet is touching the external flow, but is after a short time supposed to be overtaken by shear. The cloud cavitation is new cavitation, created by the new forces, surface tension and shear, and is thus genuine secondary cavitation. *The free shear layer between the re-entrant jet and the external flow is a so called mixing layer that results also in spreading of cloud cavitation into a large region, after some time typically into the entire shed part of the sheet*. Sometimes a non-separable mixture of primary and secondary cavitation may be expected and also if there would be no need to discriminate primary from secondary cavitation, *it is necessary to predict the total cavitation volume*, i.e. to capture both types.

Erosion by primary and secondary cavities

Figure 2 shows some generic cavitation configurations and it is noticed that secondary cavitation appears and generates erosion in virtually all cases. In the blade tip case, denoted by II, the resolution of the high-speed film at 7000 fps did not however resolve the process enough to permit a reliable analysis. In the cases classified as I the primary, almost glassy, cavity is dominating erosion generation. In case III the glassy primary cavity is still a source of erosion, but only in a small eroded patch upstream the main erosion zone. In cases IV and V erosion is generated by secondary cloud cavities only. In case V the secondary cloud is also slightly lifted above the blade surface, so the erosion is weak, despite the nasty looking cloud.

A striking observations is, that when erosion is generated by a primary cavity, it seems often to be the result of the collapse of an almost glassy cavity, rather than a massive cloud collapse, usually being associated with erosion. This seemingly controversial statement will be discussed below.

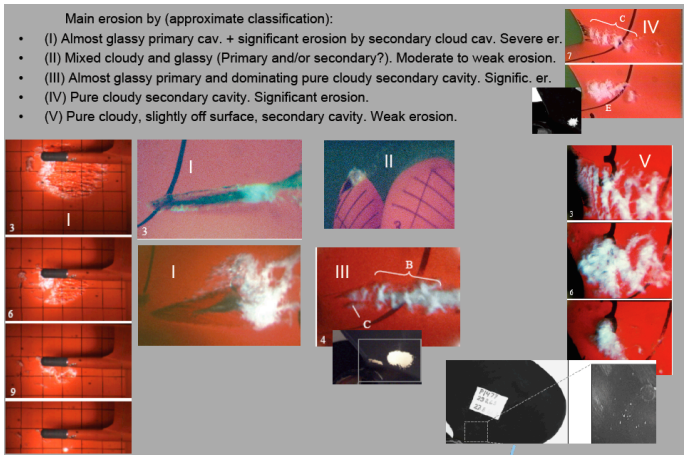

Figure 2 *Some main erosion cases and demonstration of the importance of secondary cavities. Data from the EROCAV Handbook.*

Notes on cloud cavitation and erosion

In the demonstration of erosion due to primary and/or secondary cavitation, Figure 2, it was stated that severe erosion could be generated by the collapse of glassy, or more precisely, almost glassy sheet cavities. This statement necessitates some comments. Often erosion is associated with the collapse of primarily cloud cavitation, referring to the fact that collective collapses of interacting bubbles in the cloud are shown to be very effective in focusing collapse energy into a small spot, and typically generate significantly larger collapse pulse amplitudes than singly connected cavities. These ideas are reviewed in e.g. the books by Brennen (1995) and Franc & Michel (2004).

A number of experiments with foils and propellers in the SSPA cavitation tunnel during the EROCAV and VIRTUE projects certainly confirm that cloud cavitation can generate severe erosion, but still more that the most severe erosion in a number of conditions with mixed glassy and cloudy or only cloud cavitation was generated by "almost glassy" sheet cavitation. The term "almost glassy" refers here to a glassy cavity with a small amount of cloud cavitation attached to the edge of the "focusing cavity A", Figure 3, created by shedding from the leading edge of the foil exposed to unsteady inflow.

In the EROCAV handbook any type of cavity, concentrating the collapse energy into a small region by its collapse kinematics, is called a focusing cavity. Beyond the time after which the collapse motion cannot be traced in detail with the applied recording technique the cavity is defined as a "micro cavity", supposed to continue the energy focusing in a collapse of any configuration, including also generation of microjet impacts. The details of the "micro focusing process" and transfer of energy to the solid is not resolved in the numerical or experimental data. A collapse of this type is shown in Figure 3 and Figure 4.

Typical for this class of collapse developments is also that the collapse of the glassy part of the cavity is mainly finished before the cloud starts to decrease. Due to this behaviour the collapse of the glassy part will accelerate the liquid interface that will now become the external collapse front of the cloud, and the glassy collapse determines in this way the initial conditions for the collapse of the cloud. Although the symmetry properties of the case shown in Figure 4 do not match entirely the conditions applied by Mørch (1982) in his formulation of an equation for the collapse of a cloud, his equation is applied in a discussion of a conceptual model motivating the present view of the contribution to erosion by a glassy collapse forcing a cloudy collapse, Bark et al. (2004, 2004a).

The collapse of an empty cavity of radius R, starting from rest at R_o and forced by the pressure P_o, generates at the distance $r/R \approx 1.587$ a pressure maximum that, when $R_o/R \rightarrow 0$, can be expressed as $p_{max} \approx 0.157 P_o (R_o/R)^3$. Referring to the original analysis we call this localized pressure pulse for the "Rayleigh collapse pulse" or simply collapse pulse. For a gas-filled cavity Hickling and Plesset (1964) demonstrated numerically that this pressure will in the end, when $dR/dt = 0$, appear on the cavity interface. In the present case, when there above a compressible gas also is a vapour cloud inside, dR/dt will become zero after the closure of the glassy cavity. Before that, an enhanced pressure may occur inside the cavity, due to inertia and gas compression, and force the cloud collapse.

A noticeable observation is that the small cloudy structure is continuously re-generated throughout the collapse, a point that holds for virtually any travelling sheet observed on a number of foils and propellers. The generating mechanisms may be more than one but in observations of travelling bubbles discussed later in connection with Figure 11 it was noticed that asymmetrical collapses resulted in similar re-entrant flows and shear generated tiny clouds. This is also observed in the collapse of the glassy sheet of type I in the propeller blade root region shown in the upper frame of the 2nd column of Figure 2. The final collapse of this small cloud seems to be perfectly synchronized with, or rather by, the glassy sheet, as in Figure 4.

At the slightly lower cavitation number in the frame below, 2nd column of Figure 2, also severely erosive, there is a larger cloud generated during the earlier part of the collapse of the sheet, as shown in the first 6 frames of Figure 19. The collapse of this major cloud is however significantly dispersed in space, and not very coherent with the collapse of the glassy part and the tiny cloud attached to the edge of the glassy cavity. The major cloud outside the sheet removes the paint, as does the collapse of the bubble sheet further out on the blade, and it will thus most certainly result in erosion at full scale. The glassy sheet with its internal cloud does however erode the bronze material at model tests at 9 m/s and is thus much more erosive than the cloud. For foils in unsteady inflow almost glassy cavities have been observed to create single pits in the bronze even at 5 m/s, Schöön (2000).

Comparison of the collapses of almost glassy and pure cloud cavities at all studied conditions, including rebounded fairly homogeneous cavities, indicates that the collapses of clouds are typically significantly more dispersed in space as well as in time. Single cloud collapses may be very well focused and such cloud collapses can generate collapse pulses, having frequency contents up to some hundreds kHz, and amplitudes higher, than pulses from the most violently collapsing almost glassy cavities (Examples are shown in the

EROCAV handbook). *Single collapses of clouds may thus be at least as erosive as glassy cavities, but over many cavitation cycles the cloud collapses may typically be more dispersed over a larger area compared to the glassy cavities*.

The same impression of significant dispersion of energy focusing in a single cavitation cycle is supported by the classic data of ultrasonic cavitation presented by Ellis (1955). In his pictures of collapsing, globally fairly symmetric clouds, it can be noticed development of multiple collapse centres. Benjamin and Ellis (1966) also refer to data by Knapp indicating that only one of 30 000 transient clouds resulted in pitting of an aluminium target in a water tunnel. In far from all conditions are glassy cavities perfectly focused into a single spot, but when they develop high collapse symmetry their synchronization of an attached micro-cloud can be very effective, as illustrated in Figure 4, and a "blade cutting cavitation" is a fact. Also Mørch points out that the symmetry of the cloud is crucial. Possibly is the symmetry and bubble distributions assumed in idealized models seldom reached in practice.

In all observed cases of erosive almost glassy cavities has the tiny cloud attached to the glassy cavity been present, and this has been assumed to typically enhance the erosion, *due to the potentially higher focusing collapse dynamics in a cloud*. By this assumption generation of erosion by (almost) glassy cavities is still consistent with the classic idea that erosion is primarily associated with cloud cavitation, *although, with the remark; not entirely, the most erosive configuration may be a moderate or small cloud, gaining energy from a glassy collapse, highly focused in space and time, over most cavitation cycles*. This conclusion is important at a kinematical assessment of the erosion risk, and *consideration of energy focusing by large scale cavities of* ***any internal configuration*** *is thus important, also because the large scale cavity is directly related to global design parameters.* This conclusion also indicates that a detailed simulation of the cloud development is not necessary for a still reasonably good erosion risk assessment, based primarily on kinematic analysis.

By a coherent collapse, a cavity can in principle focus an energy proportional to the entire initial cavity volume. Usually, collapses are however not very coherent throughout the collapse. Sometimes an accelerating collapse motion can be retarded for some time and loose energy. Also, the cavity may disintegrate into several weakly correlated parts, and only a small fraction of the initially available energy may be focused by the final collapse. Also acoustic interaction between nearby collapsing cavities can result in strongly enhanced pulses by focusing a very small amount of the total energy, as demonstrated numerically for two bubbles, Hallander and Bark (2002). This is still an indication of the importance to observe from which time the focusing collapse motion is effective, and not suffer from disintegration or otherwise changed collapse coherence of the cavity, or temporarily reduced collapse velocity.

In the present discussion the impression may appear that cloud cavitation is created only as secondary cavitation, but this is not the case. An example of a primary cavity of cloud type is the bubble sheet shown in Figure 19. Clouds generated by body vibration or acoustic fields are other examples.

Preliminary it is concluded that simulation of cavitation as a single fluid of variable vapour/liquid volume fraction seems reasonably consistent with the presently suggested view on how cloud and glassy cavitation interacts but the details remain to be investigated.

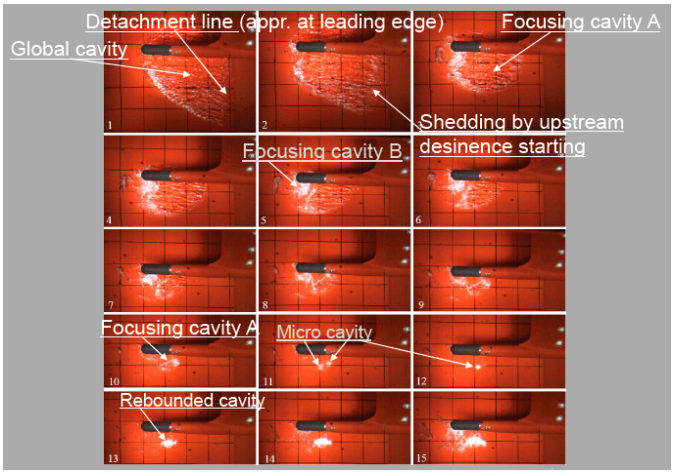

Figure 3 *Illustration of the focusing motion of an almost glassy sheet cavity, shed from the leading edge visible to the right, on a twisted foil in unsteady inflow created by an upstream gust generator. Introduction of the concepts of "global", "focusing" and "micro" cavities. Test at 5.0 m/s and σ = 0.9. The final part of the collapse is shown in Figure 4. EROCAV Handbook.*

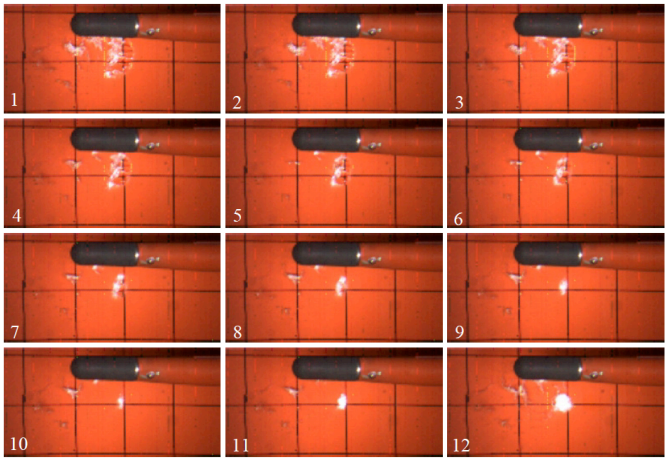

Figure 4 *Collapse of an almost glassy sheet at the same condition as shown in Figure 3 but here resolved by 30 000 fps.*

SECONDARY CAVITATION AND ITS MECHANISMS

In this section we present descriptions and ideas of mechanisms involved in generation of some types of secondary cavitation. The data are based on the experiments described in the Appendix. We start with some observations on a foil before the more complex propeller cases.

Shear due to filling of the cavity by internal jet flow

To get an idea of what is going on inside a downstream convex cavity we look first at an LES simulation of the cavitation on the twisted Delft foil, experimentally studied by Foeth (2008), with a maximum angle of attack in its centre plane, Huuva (2008). Figure 5 shows in the uppermost frame a view from

above and in the other frames views the flow in centre plane normal to the foil surface. Frames a – d are from the first cavitation period, e from the second somewhat differently developing period. The flow can be described as:

- Frame a: Filling of the downstream part of the sheet, strong shear and initial development of shedding of a single vortex cavity.
- Frame b: Filling of the middle and upstream part of the sheet and development of moderate shear.
- Frame c: Filling of the far upstream part.
- Frame d: Development of free shear layer in this region and after some time a cavitating vortex.
- Frame e: The thin re-entrant jet does not touch the external flow until far upstream in the cavity.

The filling of the cavity is the result of re-entrant jets from behind as well as "side-entrant jets" from the sides, Foeth (2008), and it is obvious from the frames a – e that the shear developing between the filling flow and the external flow can change over time and with the jet conditions. In frames a and b, the shear is weak and there is still some vapour in the shear layer. In frames c and d, the shear has increased and cavitating vortices are developing, not fully resolved however.

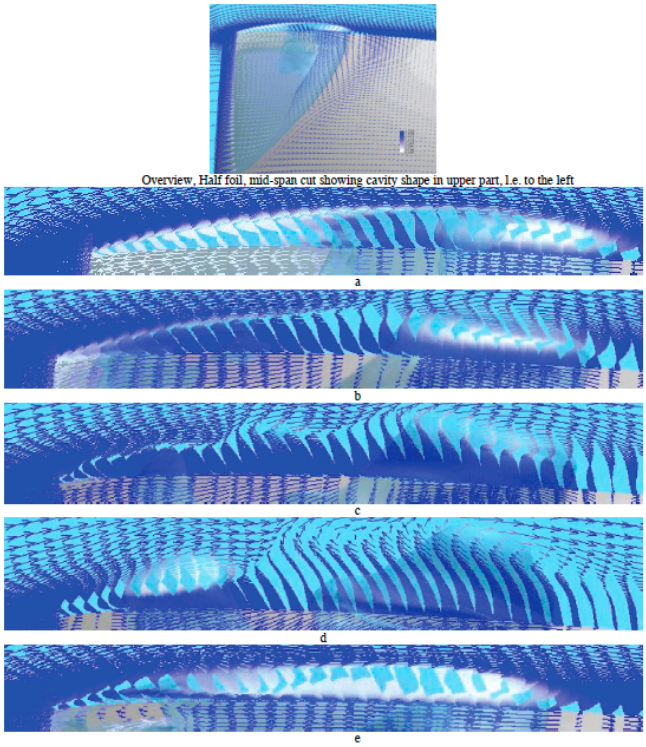

Figure 5 *LES-simulation by Huuva (2008) of cavitation on Twist 11. Flow from left. The leading edge is the dark vertical line far to the left in the frames. The uppermost overview frame shows the half spanwise view of the foil surface and the velocity vectors in the innermost cells with the vectors coloured by the liquid volume fraction, pure vapour = white. The downstream convex line is the closure line of the cavity. A bit upstream this line the side-entrant liquid flow is visible. In the vertical centre plane the cavity thickness profile is visible. The lower frames a-e are magnifications of the vertical centre plane, showing the cavity profile and the velocity field inside and outside the cavity in this symmetry plane. See also Foeth 2008.*

With a different foil in forced oscillation, three similar states are observed, side by side, due to 3-D effects, in Figure 6. The following observations are made:

Figure 6 *Three behaviours of re-entrant jets. (z = 10 along the uppermost chordwise black line, x = 0 at leading edge, line spacing = 20 mm in x and z directions). (5 m/s, cavitation number σ = 1.21, oscillation freq. = 14.4 Hz, ampl. = 3°, mean angle = 7°).*

1. Around z ≈ 60 mm the side entrant jet from above is dominating early in the process and has filled the cavity entirely so that the liquid inside the cavity touches the external flow. A significant shear thereby occurs and typically one or two significant parts of the sheet are finally shed. Due to the continuous strong shear and mixing the shed part is cloudy as far as can be observed from the outside. The jet, later dominated by the upstream moving re-entrant jet, is moving all the way to the leading edge, continuously creating strong shear. When the far upstream part of the sheet is entirely filled by the re-entrant jet, the fluid becomes pure liquid and fully transparent for some time - until tiny cavitating spanwise vortices finally are formed in the free shear layer slightly outside the foil surface.
2. Around z ≈ 100 mm the side entrant jet from below mainly contributes to filling of the sheet. Due to the less convex sheet in this region the jet from below is weaker and hence the filling and shear here is less developed. The shear starts in the mid part of the sheet and is moving to the leading edge, but not until the far upstream region is the shear strong enough to result in some rather weak vortex formations in the mixing layer. No early shedding.
3. Around z ≈ 80 mm the internal jet is mainly an upstream moving re-entrant jet, not in this case thick enough to fill the downstream and mid part of the cavity, which thus stays nearly glassy up to x ≈ 20 mm. Further upstream the jet is however touching the external flow and finally the sheet is completely filled in the far upstream region. Strong shear develops in the mixing layer, lifted from the foil surface to a distance corresponding to the cavity

thickness. *The cavities created in the mixing layer (in all three cases) are genuine secondary cavities*, and a minimum of entrainment of vapour from upstream cavitation is expected to influence the growth. In this type of condition the shed cavity is often partly glassy.

In particularly the second case is the generation of genuine secondary cavitation assumed to be weak, it is more of a mixing process. In the third case there is no doubt that secondary cavitation is generated by the shear. Here the cavitation starts in the shear vortices, but if the liquid is weakened by cavity remains from an upstream cavity, secondary cavitation may be created directly due to the shear, as may be the case in the first frames in Figure 13.

Observations of shear induced vortex cavities

The next issue is the interaction between the so created vortex cavities. It is noted from the EROCAV handbook that merging is a key mechanism for formation of erosive vortex group cavitation, Figure 7. The merging process on the foil is confirmed at a number of conditions, and on the propeller P1477 as well, Figure 8.

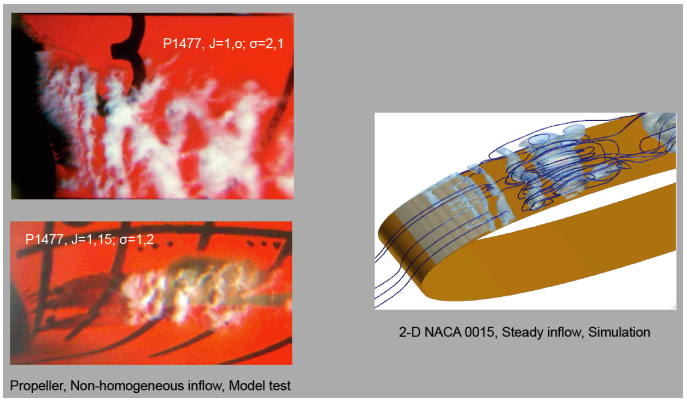

Figure 7 *Vortex group cavitation downstream a mainly glassy sheet on a propeller during model testing and simulated by Large Eddy Simulation, LES, at a 2-D foil with some streamlines indicated.*

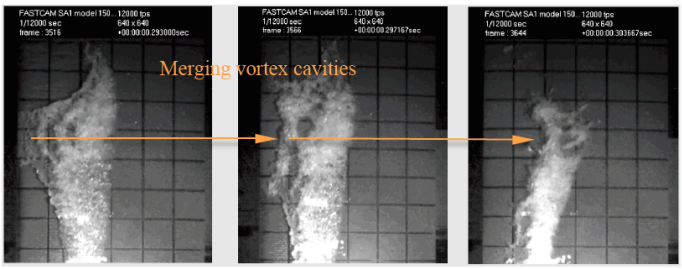

Figure 8 *Merging of vortex cloud cavities at an oscillating foil. Flow from left, 5.0 m/s, σ = 1.21, mean angle of attack 5°, oscillation amplitude 3°, oscillation frequency 13.4 Hz.*

Two main mechanisms of merging are identified:

1. Merging of cavities due to variable vortex transport velocity, a behaviour observed over a large span of scales.
2. Merging due to growth of the cavitating part of the vortex.

The mixing generated already by liquid vortex formation, may be significantly enhanced by the vortex cavitation. The preliminary impression is that large scale merging is similar to an early phase of a vortex layer development due to a Kelvin-Helmholtz instability, see e.g. Corcos *et al*. (1976) and Patnaik *et al.* (1976). However it is also clear from the simulations by Huuva (2008) that there can be a significant backflow reaching far upstream, due to separation or cavitating vortices in the downstream region. A correct simulation of this backflow is important for judging the risk of erosion, also because the backflow typically lifts secondary cavitation from the body surface. The following effects of the merging and mixing are particularly pointed out:

- The cloud becomes more homogeneous, and thus disposed to perform a well synchronized energy focusing collapse.
- The details of the merging seem to control the rotation of the merged vortex cloud, a motion influencing the collapse forcing pressure.
- The merging implies a cascading of cavity collapse energy towards a single coherent structure, a development that can increase the risk and amount of erosion, or reduce the risk.

Secondary cavitation induced by asymmetric collapse and rebound motions in non-homogeneous flow fields

The collapse motion of sheet cavities, attached or travelling, is a significant source of secondary cavitation. An example is the spanwise collapse of a sheet attached to the leading edge as shown in Figure 9. A secondary spanwise vortex cavity "replaces" the disappearing sheet. The contribution by rebound by elastic compression to this secondary cavity is assumed to be small, because virtually no gas can be locked into a disappearing volume.

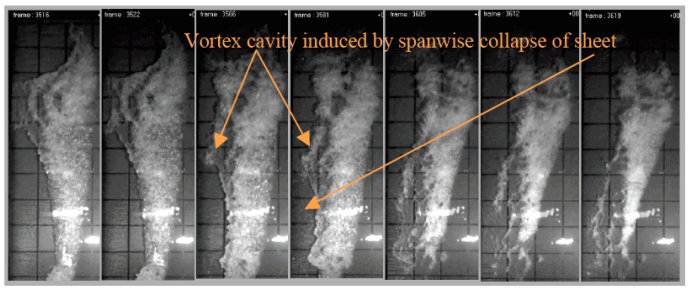

Figure 9 *Spanwise collapse of a glassy sheet attached to the leading edge (the left edge in each frame). 5.0 m/s, σ = 1.21, mean angle of attack 5°, oscillation amplitude 3°, oscillation freq. 13.4 Hz.*

An extension into a travelling sheet is shown in Figure 10. Although the collapse in a sense is fairly symmetrical and focusing, there are also asymmetries, e.g. the partly "open" downstream edge moving only slightly upstream during the collapse – compared to the differently appearing upstream edge. In frame 4 the minimum captured size of the sheet cavity is shown. In this case there is evidence of a fast, compression rebound that however is mainly finished in frame 6. The first downstream spreading is typically faster than motivated by the advection. Rebound in the downstream area may be enhanced due to cavity remains being left there during the upstream moving collapse. Rotation of the rebounded cloud can be noticed from frame 9, or earlier. Particularly the rotation indicates that compression rebound is not the only source of the rebounded (secondary) cavitation.

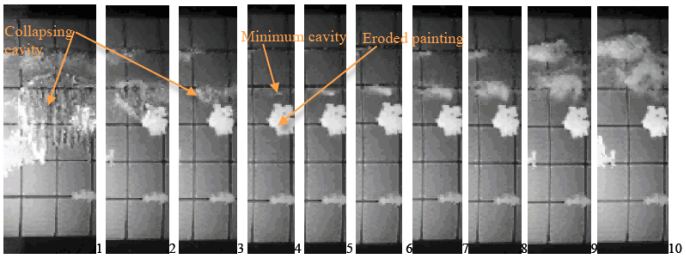

Figure 10 *Development of secondary cavitation downstream a collapsing sheet. Flow from bottom to top. The paint eroded away (the light patch approx. at the midchord position) was not a result of the shown cavitation. Recorded at 40 000 fps. Suction side, 5.0 m/s, σ = 1.02, mean angle of attack 7°, oscillation amplitude 3°, oscillation frequency 18.4 Hz. The frame numbers in the video sequence of the shown frames 1,..10 are: 400, 470, 490, 499, 500, 503, 510, 520, 560, 600. The interval for one unit step of the number is 1/40 000 s.*

Development of certain collapse asymmetries due to inhomogeneous pressure/flow field was studied for travelling bubbles on the oscillating foil, Figure 11. It was noted that the collapse motion of initially almost half spherical travelling bubbles remained almost cylindrically symmetric (with some flattening on the bubble top) if the bubble collapsed in the mid-chord region with an almost zero stream-wise pressure gradient. At collapses further downstream, where the stream-wise pressure gradient was steeper, a significant flattening started from downstream, developing into an inward buckling or intrusion, filling the bubble from behind. During the filling of the bubble a part of it was cut off and a tiny cloud developed, due probably to shear between the filling and the flow outside the bubble.

The filling flow is in principle a re-entrant jet but its initiation is slightly special – the travelling cavity enters a region of increased pressure, compared to creation of a stagnation pressure behind a cavity mainly attached to the foil. While the ordinary re-entrant jet is usually thin in the case of a sheet, the filling flow in the bubble is thick, more like the filling by an upstream moving collapse of a sheet having an open closure region. The broken off part as well as the remaining part of the bubble had a noticeable rotation after the rebound.

Particularly the cut off of a part of travelling bubbles on headforms was reported by Ceccio and Brennen (1991) claiming that ", the rough bubble or group of bubbles which is formed after collapse is sheared by the surface flow…", a statement confirmed by the present observations. Shear deformation of particularly rebounded bubbles seems also to exist in the data shown by van der Meulen et al. (1988).

Collapses having the present type of asymmetry seem thus to end up in secondary cavitation having a significant rotation after the collapse of the primary cavity, and *it is concluded that the reason for the rotation, shear motion and related cloud generation is the asymmetry developing during the collapse*. Interaction between a pure collapse induced flow and the global flow is assumed to be important. Simple rebounds controlled by elasticity of liquid and gas are then transformed into more complex "generalized rebounds", of which the far left lower frame in Figure 1 is an example. Much of the observed behaviour follows from the analysis of the Kelvin impulse originally made by Benjamin and Ellis (1966) for prediction of the formation of collapse asymmetry and microjets directed towards a body surface. Although not a part of the theory, viscous shear can often be expected to appear due to the predicted jets.

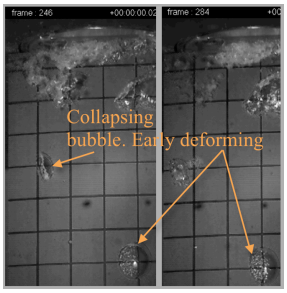

Figure 11 *Travelling bubbles on oscillating foil. Flow from right to left. σ = 0.72, Velocity: 5.1 m/s. Time between the frames is 167 μs.*

Vortex group cavitation due to an upstream moving collapse of an attached sheet – Propeller studies

The vortex group cavitation is, besides rebounded cavitation, the most important type of secondary cavitation. Below are presented the developments of the vortex group cavitation during a systematic variation of the condition that takes the secondary cavitation from almost non-erosive to the dominating or only erosive cavity. This variation will also demonstrate how erosion generation is shifted from almost glassy to cloudy cavitation.

As shown in the Appendix the propeller P1477 was operated in inclined flow, with the shaft downstream the propeller, i.e. in a simple but varying wake. We focus on a rather narrow sheet cavity, that at the present condition with the advance coefficient $J = V_A/(nD) = 1.0$ and the cavitation number $\sigma = 2.1$, has developed slowly from a large sheet covering a significant part of the blade, (V_A is the advance velocity, n the rotation frequency and D the propeller diameter). Towards the end this sheet becomes rather 2-D. An overview of the final development is shown in Figure 12 and Figure 13.

At $J = 1.0$, corresponding to a higher than design load, the cloud was slightly lifted from the blade surface, and the nasty looking cloud generated then only a few pits in the soft paint, interpreted as weak erosion, case V in Figure 2. There are no indications of erosion due to the collapse of the primary cavity, i.e. the mainly glassy sheet. This result is confirmed by repeated tests. From Figure 12 we observe the main features:

- Early in the development, frames 1-3, the sheet has been shedding larger clouds due to re-entrant jets. Later on, the remaining sheet performs an upstream moving collapse, the character of which is supposed to control the generation of the vortex group cavitation downstream the collapse front. This vortex group cavitation is classified as pure secondary cavitation. The sheet and the vortex group have some 2-D main character, but the details are highly 3-D.

- The primary cavity is a glassy sheet, permanently attached to the leading edge and collapsing by upstream motion of a mainly open closure region.

- Rather late during the upstream moving collapse vortex group cavitation is generated downstream the primary cavity.
- The individual vortices in the vortex group merge into a cloud that may end up in a single homogeneous cloud cavity but more often in 2 or 3 separate clouds that finally are transported downstream and collapse.
- The collapse of each cloud can be very well focused, or dispersed into a few parts. Individual cloud collapses are typically followed by very fast rebounds and are classified as erosive, if they had occurred close enough to the body surface. Over a number of blade passages the collapse points are rather or significantly scattered.

Detail observations from Figure 12 and Figure 13:

1. There may still exist some late but marginal re-entrant jet flows. The cavity closure region is estimated as mainly "open", typically with an "overshoot" tail, from which shedding of small structures may be observed, similar to the numerical simulation in Figure 14.
2. The thin sheet of bubbles, the overshoot tail of the glassy sheet shown in the first frames of Figure 13, may be an entrainment of cavitation remains from the sheet, as indicated in Figure 14, rather than an excitation of nuclei by shear. It is noted from many films that vortices can roll up quickly in this sheet, but sometimes it takes some time.
3. The vortex cavities are created during the collapse of the sheet and some growth and merging may occur early. The massive growth and merging of the vortex group cavitation starts not until the collapse of the sheet towards the leading edge is finished, frames 998-1010 in Figure 13.
4. The merging is forced partly by cavity growth and by a mixing process, similar to an early Kelvin-Helmholtz development, with the vortices travelling at different velocities and catching each other.
5. When the sheet collapse reaches the leading edge three main alternatives typically happen:
   a) A: The collapse front, i.e. the closure line, reaches the cavity detachment line close to the leading edge and the sheet disappears without any visible trace.
   b) B: The collapse front moves spanwise along the leading edge, thereby inducing a spanwise vortex cavity along the leading edge, frames 994 - 1000 in Figure 13, similar to Figure 9.
   c) C: The collapse front converges locally towards a point close to the leading edge, and a tiny compression rebound occurs, as shown in the lower edge of frames 992 - 994 in Figure 13. No erosion is noted due to these spatially dispersed collapses.
6. In all cases A, B and C the massive growth of the vortex group cavitation starts in the far upstream area where the sheet disappeared, and spreads downstream to the entire vortex group. The growth and spreading is most substantial when already secondary cavities are generated by a fast primary collapse, i.e. in the cases B and C. Some early growths can be rather fast and the growing clouds have a strong rotation and finally reach a significant size. Contribution from a compression rebound is not excluded, although it often starts from a rather slow collapse. The strong rotation indicates creation of also a vortex formation due to asymmetry.
7. There are indications of a "collapse wake", of some structure. For example does the vortex cavity extending mainly vertically downward from the crossing of the radial and tangential black marking lines, frames 994 – 1004 in Figure 13, not move relative the blade until the frames 1010 – 1020. Close to the collapse front it is even possible to find vortex cavities that move upstream.
   Because the shed vortex is created between the free stream velocity and the very local collapse flow moving upstream, the transport of the shed vortex is expected to, at least initially, be slower than the free stream velocity.
8. When the secondary cloud cavity is swept downstream by the recovering flow, a new sheet grows during a short time from the ordinary detachment line in the leading edge region, frames 1090 and 1120 in Figure 13.
9. As far as can be resolved the character of the vortex cavities is a true bubble cloud, temporarily with the bubbles more concentrated around the vortex core. The mixing by the vortex interaction appears to be very effective, but still the bubble distribution is mostly rather inhomogeneous in the collapse phase, and the focusing of collapse energy is typically dispersed into a number of points as shown in frame 5967 from a different recording. Note however the perfect focusing to a point in frame 1132 of the cavitation cycle shown in Figure 13. This collapse has a fast and substantial compression rebound, frames 1138 and 1158, and is assumed to be erosive, if it had occurred repeatedly in the same point on the blade surface. Usually, in this condition, parts of the cloud collapse further downstream, outside the frame, and the dispersion in space and time is substantial, an observation confirmed also by the paint test that indicated weak erosion only.

Compression rebounds are expected to initially be very fast, and still at 90 000 fps the cavity typically "explodes" during the first one to three frames. A compression rebound also requires a coherent collapse, and typically such rebounds start from a single point or a line. The observed cases are more complex, with rebounding of a number of isolated parts. Some compression rebounds seem however to occur close to the leading edge. Certainly they are dispersed, but still it is slightly surprising that they do seem to not generate any erosion.

We summarize as a **preliminary hypothesis for parts of the development of vortex group cavitation**:

1. Vortex cavities are generated and shed due to filling flow and shear action in the "overshoot" region, (Figure 14), as suggested by Foeth (2008).
2. Towards the final filling of the sheet permanent gas inside may be compressed, although some of it may escape downstream in the shear region as can be imagined from the simulations in Figure 14 and Figure 5, a, b. At the same time the shear in a short free shear layer is built up, and a

last secondary vortex cavities may be created, as shown in the filled region close to leading edge, far left frames in Figure 8, Figure 9. Such a shear/vortex cavity appears also a bit downstream the leading edge in Figure 5, d.

3. The filling flow combined with the flow outside the sheet constitute towards the end of the collapse a concentrating vortex that will capture what remains of the primary sheet, that now also may approach the onset of a compression rebound. The rebounding is enhanced by the vortex motion. If a shear induced vortex cavity, according to previous point, was generated this may be captured as well, and the thick, *strongly rotating cloud formations starting far upstream* in frames 1000-1020 in Figure 13 may be formed.
4. To what extent the two suggested "sources" contribute to a generalized rebound as shown in frames 1000-1020, and if the rebound occurs at all, depends on the intensities of the components. A fast collapse generates a stronger vortex and a stronger gas compression.

The described development, including the final collapse vortex visible also in the most upstream region, is consistent with the analysis of the Kelvin impulse made by Benjamin and Ellis (1966) for the asymmetric collapse.

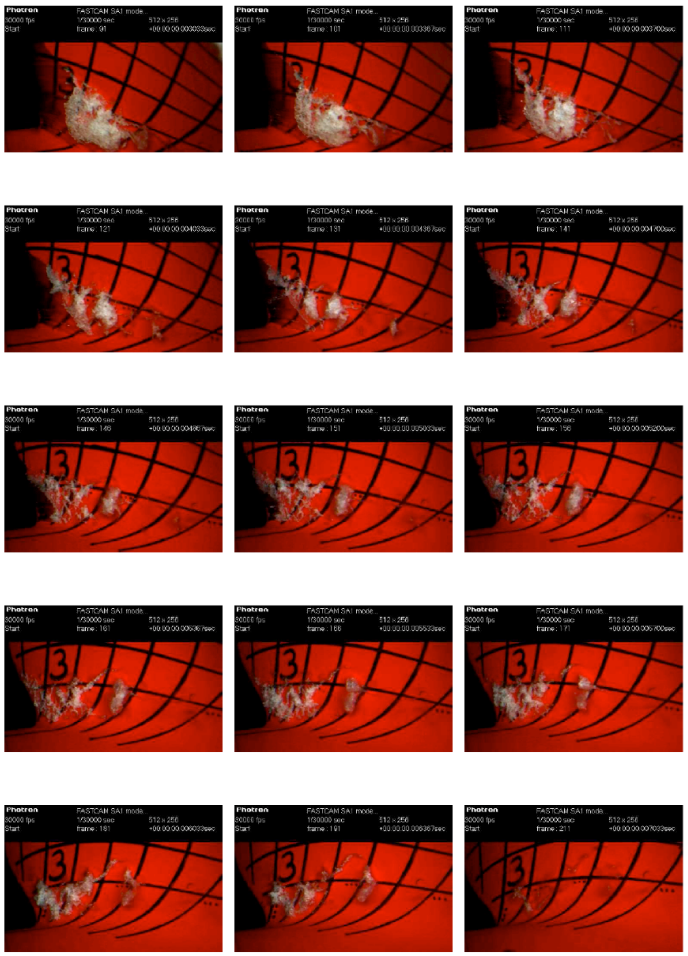

Figure 12 *P1477, J = 1.0, σ = 2.1. Velocity: 8.0 m/s.*

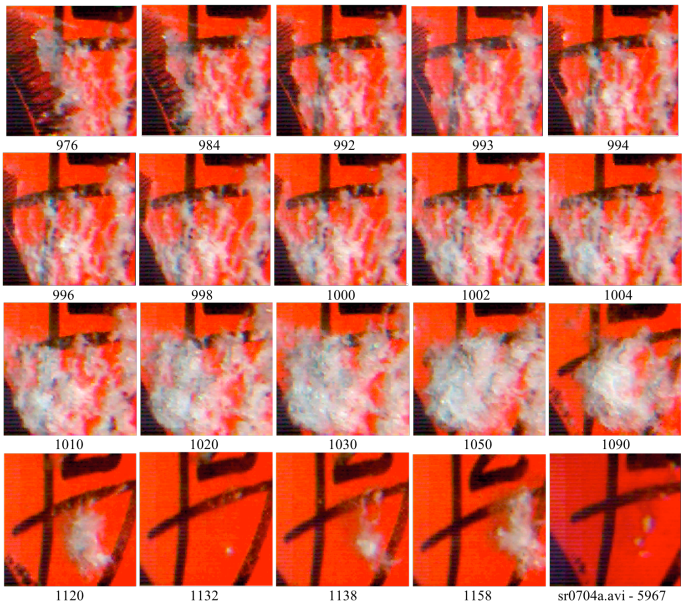

Figure 13 *P1477, J = 1.0, σ = 2.1, 8.0 m/s. Video: 90 000 fps. Leading edge to the left. Selected frames for end of sheet collapse and growth and merging of vortex group cavitation. Frame numbers are from the video recording and the interval due to one unit step of the number is 1/90000 s. Last frame illustrate is taken from a different recording of the same condition at the same event, and compared with 1132, shows a typical scatter of focusing of the final collapse. Typically collapses occurred to the right of the present frame as well.*

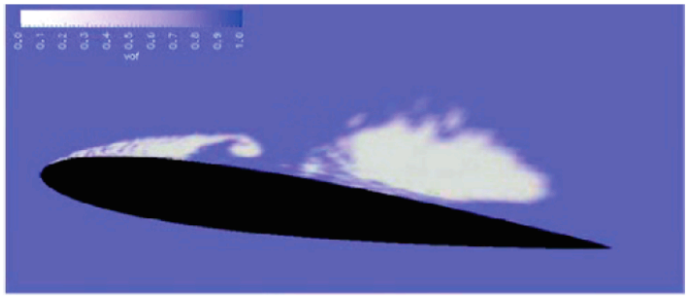

Figure 14 *2-D sheet cavity with "open" closure region, a slowly penetrating thick re-entrant flow and an overshooting vapour tail being entrained in to a vortex. The shown view is from the second cavitation cycle. A thin re-entrant jet has travelled far upstream into the sheet and created the break-off of the large rotating cloud cavity visible downstream. The thick re-entrant flow is induced by the rotating cloud and this reversed flow generates a temporarily upstream moving collapse, having some similarity with the propeller case in Figure 13. LES – simulation by Wikström et al. (2003).*

Vortex group cavitation due to travelling sheets

We consider first P1477 at $J = 1.15$, the design loading, and $\sigma = 1.3$ as shown in Figure 15 and Figure 16. The upstream edge of the glassy sheet is now moving slowly and slightly downstream during the collapse. The collapse motion of the glassy sheet becomes then more symmetric and violent, resulting in a more pronounced compression rebound and a corresponding small patch of paint removal, case III, Figure 2. The dominating paint removal slightly downstream is however caused by the group vortex cavity, i.e. the secondary cavity. The specific observations for the loading at $J = 1.15$, are:

1. Although the sheet is not permanently attached to the leading edge, the upstream collapse motion is still the dominating motion. Late during the collapse the open closure region of the cavity is moving upstream with a (phase) velocity relative the blade being 2 - 5 times the downstream flow velocity. Downstream the closure region there are shed vortex cavities being almost stationary relative the blade or, close to the shedding position, move upstream with a velocity that occasionally approaches the local flow velocity, but typically is lower.
2. Figure 16 shows the combined downstream and upstream moving late part of the collapse. In frame 8526 two vortex cavities shed from the upstream moving closure region of the mainly glassy sheet are visible just below the arrow. In this frame they are close to their minimum sizes. The *erosive* collapse of a part of the glassy cavity was ended just before frame 8526 (the horizontal white strip below the arrow, on the upstream paint removal resulting from the glassy collapse, case III Figure 2). The early rebound of the glassy part, 8526-8529, is assumed to be dominated by elastic compression. It spreads first upstream and not until 8530 is a clear rotation visible. It is indicated by the film that the pulse from this rebound, by acoustic interaction, further reduces the sizes of the two vortices and thus enhance their rebound, first visible in frame 8528. From frame 8529 the growth spreads downstream, significant rotation and merging develops and around frame 8550 the downstream transport velocity of the now merged and homogenized cloud increases.
3. From Figure 15, it is noticed that the group of vortex cavities is partly suppressed during most of the collapse of the glassy cavity, although there is a tendency for the medium downstream vortices to grow slightly. The main growth, of which a part is seen in frames 8530 – 8550 in Figure 16, spreads downstream from the collapse point, frames 2415 – 2425 in Figure 15.

Summarizing the observations and comparing with the attached sheet it is clear that the glassy collapses are now at least more repetitive and possibly also individually more focused. The compression rebound of the glassy cavity may initially be more dominating in this condition but otherwise the preliminary hypothesis from the previous condition holds. Considering the observed collapse induced upstream vortex motion and its expected interaction with the inflow, it cannot be excluded that a free shear layer extends some distance downstream the shedding position and contributes to further growth, i.e. energy gain of the vortex group, and homogenization of the cloud. It is **added to the preliminary hypothesis** above that:

1. An early rebound of shed vortex cavities can be suppressed by the collapse pulse from the primary cavity.
2. The durable and extensive growth of the vortex group may be enhanced by the rarefaction phase of the rebound pulse following after the positive part of the collapse and rebound pulse from the glassy cavity.
3. After also this pulse has faded there is an indication (a short re-growth of the primary sheet at l.e.), as in the previous case as well, that the recovering flow may support a growth of the vortex group cavitation for some time.

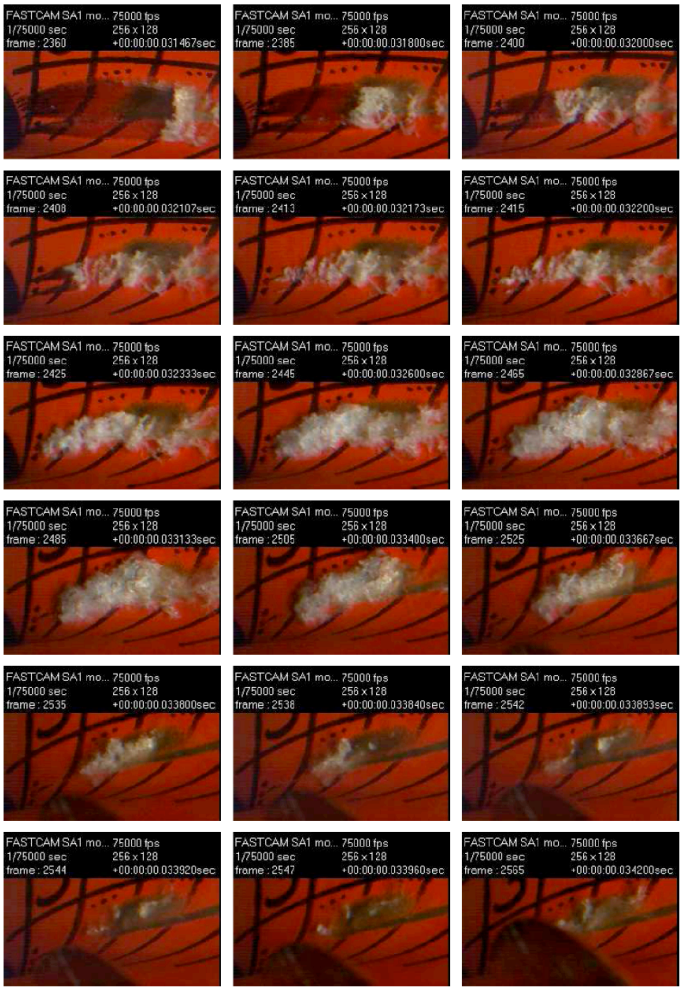

Figure 15 *P1477, J = 1.15, σ = 1.3. Velocity: 9.0 m/s.*

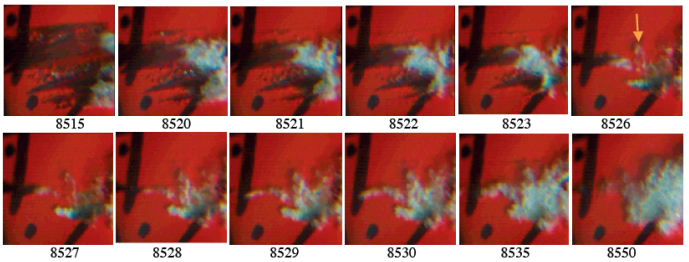

Figure 16 *P1477, J = 1.14, σ = 1.3, 8.9 m/s. Video 90 000 fps. Leading edge to the left, outside the frame. Selected frames showing the end of sheet collapse and growth and merging of vortex group cavitation. Frame numbers are the numbers in the video recording and the time interval for one unit step of the number is 1/90 000 s.*

Erosion dominated by the collapse of a travelling sheet

By lowering the cavitation number to σ = 1.0; 0.9 and 0.8, still at J = 1.15, the primary cavity is transformed into a dominating almost glassy, or at σ = 0.8 a mixed glassy and cloudy, travelling sheet cavity. Early in the development of these narrow sheets in the root region, particularly at σ = 0.9 and 0.8, there are also re-entrant jets creating shear and small or medium scale shedding of cloud formations in the downstream part. At σ = 0.8 the downstream cloud is more extended and there is also a sheet of bubbles interfering with the glassy sheet, and close up inspection is needed to understand whether the

final part of the collapse of the primary cavity is dominated by the glassy or by the cloudy structure. Overviews of the development after formation of transient focusing cavities are shown in Figure 17, Figure 18 and Figure 19.

At $\sigma = 1.0$ and 0.9 severe erosion is created by the almost glassy primary cavity (case I, 2nd row, upper frame, $\sigma = 0.9$, Figure 2) and significant or strong erosion by secondary cavitation (a mixture of compression rebound and vortex group cavitation). At $\sigma = 0.8$ the erosion by the almost glassy primary cavity is severe (case I, 2nd row, lower frame, $\sigma = 0.8$ Figure 2).

In summary the following observations are made for the last three conditions:

1. The almost glassy travelling sheet, rather narrow, has a mainly open closure region during the fast part of the collapse.
2. There is a significantly disturbed flow, a "collapse wake", downstream the open, fast upstream moving closure region. Close to the cavity the upstream velocity of the shed vortices may approach the velocity of the wetted flow relative the blade but is typically lower.
3. The collapse of the almost glassy cavity is extremely well focused towards a point or short line, and the rebound, probably dominated by compression, is violent.
4. The cloud formation in the mainly glassy cavity occurs in the closure region and is continuously regenerated, as it seems by shear in the closure region as shown in Figure 14.
5. At $\sigma = 0.8$ a sheet of small bubbles is *directly generated as a cloud*, Figure 19, outside the innermost radial line, $r/R = 0.3$. The bubble sheet collapses as a pure cloudy sheet, with slightly more dispersed focus, but otherwise with similar kinematics as the glassy sheets. Bubbly sheets typically occur at full scale and the present observation indicates that the collapse kinematics in such configurations may be similar to the glassy case, an issue that however needs to be further studied.
6. A mixed glassy and cloudy collapse can be observed at $\sigma = 0.8$. The cloud occupies finally a large part of the glassy cavity, and they collapse together, but still the cloud collapse appears to be less focused than the glassy.
7. Also these conditions demonstrate the existence of acoustic interaction, of similar type as shown in Figure 16.

Possible mechanisms of rebound of vortex group cavities

The growth of the vortex group is spreading downstream from collapse position of the primary cavity and the last growing vortex cavity is shed far before the final collapse of the primary cavity. The early shed cavity is initially therefore exposed to an early part of the pressure induced by the collapse of the primary cavity. After shedding the cavity may then be forced by this early part of the collapse pulse to make a first moderate collapse and rebound, close to the still collapsing primary cavity. Later, the shed cavity seems typically also to be forced to a second collapse and rebound by the final high amplitude part of the collapse and rebound pulse from the primary cavity.

Possibly is the final positive part of the collapse and rebound pulse strong enough to force the shed cavity to collapse and rebound, and the rarefaction phase of the rebound pulse of sufficient amplitude and duration to enhance the massive growth of the vortex group cavitation. In addition also the pressure in the recovering flow may support a growth, early or when the positive collapse and rebound pulse fades – it is at least at $\sigma = 1.3$, $J = 1.14$, low enough to support growth a new sheet at the leading edge for a short time. Particularly at $\sigma = 0.9$ and 0.8, $J = 1.16$, the pressure over the blade is also low everywhere, and a small disturbance may be sufficient to excite cavitation. It is noted that the downstream spreading of the vortex cavity growth is weaker at $\sigma = 2.1$, $J = 1.0$, a condition with weaker collapse and elastic rebounding of the primary cavity. Careful simulations seem necessary to capture and unfold these processes controlled, as it seems, by multiple pressure sources.

In cases with very fast and symmetric collapses of the primary glassy sheet the rotation of the rebounded cavity appears to be fairly small. The upstream as well as downstream cavity edges then typically move towards the collapse point with velocities significantly higher than the global flow velocity. The rotation induced by asymmetry of the final part of the collapse is then expected to be small and the rebound would be more controlled by elastic compression. Still however the collapse and rebound pulses, and the recovery of the flow, seem to influence the massive rebound of suppressed secondary vortex cavitation downstream the elastically rebounding primary cavity, Figure 17 and Figure 18.

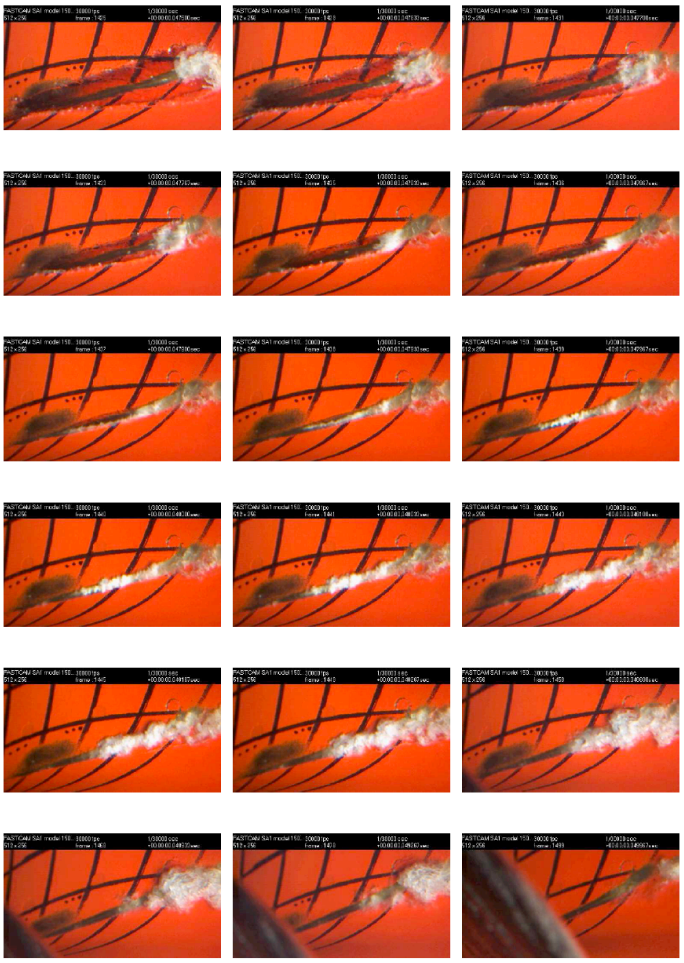

Figure 17 *P1477, $J = 1.15$, $\sigma = 1.0$. Velocity: 9.0 m/s.*

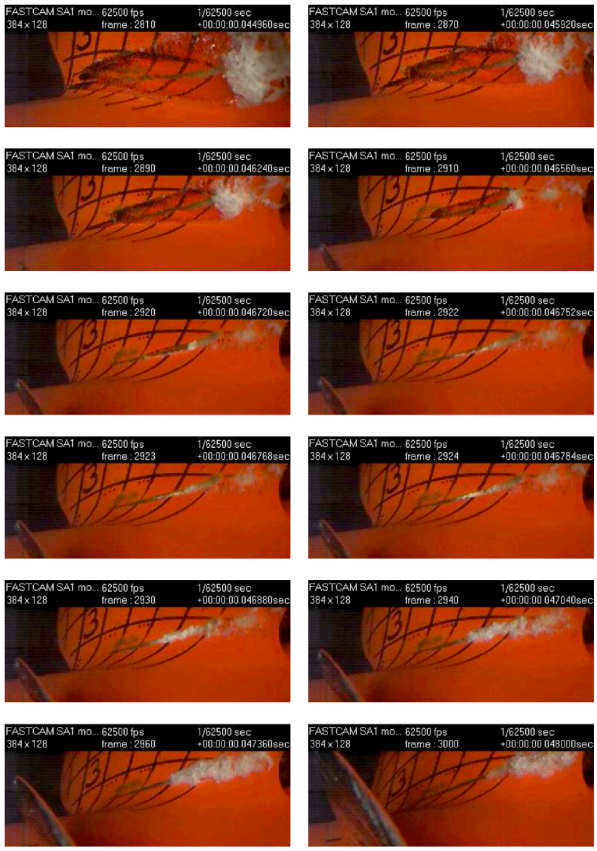

Figure 18 *P1477, J = 1.15, σ = 0.9; Velocity: 9.0 m/s.*

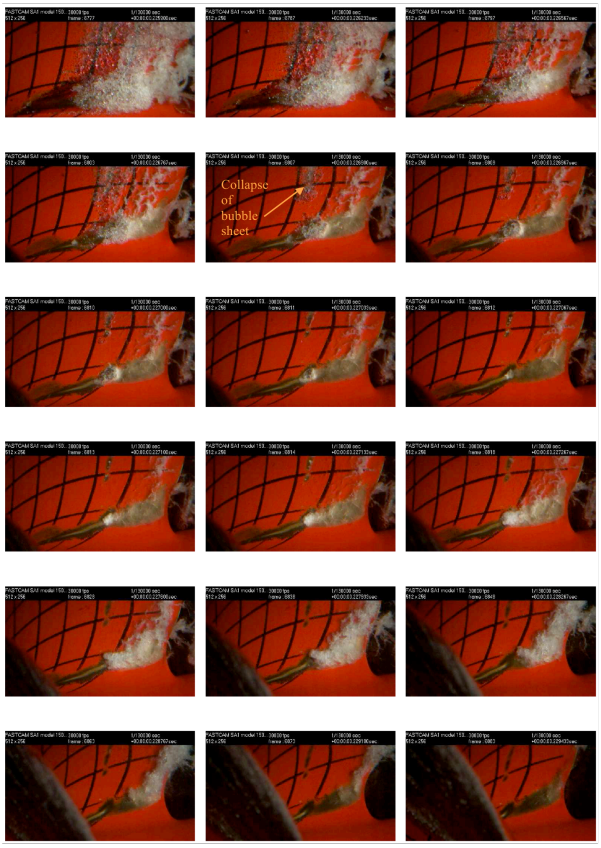

Figure 19 *P1477, J =1.15, σ =0.8; 9.0 m/s. A bubble sheet is created as primary cavitation radially outside the root cavity.*

Hypothesis for development of vortex group cavitation

We summarize the vortex group cavitation as:

- It is a delayed, massive, synchronized growth and merging of vortex cavities, created by the asymmetry that typically occurs in collapse motion of a primary sheet cavity, due partly to interaction with the main flow. The creation of the vortex group cavitation may start within the sheet but continues downstream.
- The process may be mistaken for being a simple compression rebound but is rather a *"generalized rebound"* still possibly often controlled by compression of cavity content and the liquid, but as suggested above, also influenced by generation of vortex motion due to asymmetry of various origins, viscous shear, hydrodynamic vortex interaction and acoustic interaction between the primary cavity and the vortex cavities.

Merging the impressions from the examples discussed above we suggest finally the following general hypothesis about the development of vortex group cavitation, still preliminary, due to incomplete data and analysis:

1. According to the theory of the Kelvin impulse, Benjamin and Ellis (1966), any asymmetry occurring in the flow/pressure field, induced by boundaries or applied flows in which the collapse of a cavity occurs, results in an asymmetric collapse motion. The so generated collapse asymmetry, sometimes approaching a jet-like flow, also supports formation of vortex motion. Depending on the geometry of the asymmetric collapse motion the vortex formation can be distributed and *redistributed* in different ways, *e.g. by the action of viscous shear between a jet and the flow outside the cavity*. The induced asymmetry and shear may extend also outside the cavity. The final result will be generation and shedding of one or more vortices, cavitating or not, in the closure or collapse region.
2. The completion of the asymmetric collapse of the sheet may generate, above some separately shed shear vortices, a main vortex that captures the compressed gas/vapour in the primary cavity, and possibly some nearby secondary cavity as well. *The so created far upstream secondary merged cavity may rebound, in a generalized sense, due to the combined, or one single, effect of compressed gas and liquid, and the vortex motion*. Depending on the relative importance of fluid compression and vortex motion more or less significant rotation occurs. (This explains e.g. the spanwise secondary vortex cavities due to spanwise collapses in Figure 9 and Figure 13).
3. Entrainment of cavity remains from the primary cavity into the secondary vortex cavities is supposed to be important.
4. In *an accelerating sheet collapse*, a positive local collapse pulse develops close to the collapsing cavity, in accordance with the Rayleigh equation and the boundary condition on the body surface. This pressure is supposed to suppress cavitation in shed vortices. Mild collapse and rebound of shed cavitating vortex cavities may occur due to this early part of the collapse pulse from the primary cavity.
5. If the collapse of the primary cavity ends with a strongly accelerated rebound, the suppression of shed vortex

cavities can be *significantly enhanced* for a short time, by the rebound pulse.

6. When the rebound of the primary cavity retards, a weak negative rebound retardation pulse, a rarefaction pulse of long duration, replaces the short final collapse and rebound pulse. The vortices, having possibly gained further energy by shear downstream the primary sheet, *are then exposed to a lower pressure and a significant growth of the shed cavities* may follow, possibly enhanced by a still, for some time, low pressure in the recovering flow as well.
7. Due to growth and variable transport velocity, the cavitating shed vortices will typically *merge, and a mixing into a more homogeneous cloud occurs. This mixing is assumed to be the mechanism for transforming typically the entire shed vapour volume into cloud cavitation*.
8. When the collapse and rebound is over and the entire flow recovers, it may, as assumed above, for some time support the vortex cloud, but particularly a re-growth of a new primary sheet at the leading edge for a short time. Although specifically noted at the present conditions this effect is stated to be a general trend of the recovering flow.

Further experimental and numerical studies may bring more precise statements but we assume that the character of vortex group cavitation as a balance between different mechanisms depending on the cavitation condition will remain. Remain will also the conclusion that a simulation aimed for advanced analysis of the risk of cavitation erosion has to capture vortex group cavitation, as well as the energy focusing by glassy *and* cloudy cavitation.

CONCLUSIONS

In this paper, we discuss the nature of erosive cavitation, some main mechanisms of the phenomena and the implications this have on the possibilities of doing numerical erosion risk assessment, implications which often are relevant also when setting up and analysing experiments. In particular we emphasise what we have chosen to call secondary cavities, arising as new cavities due to a flow field modified by the dynamics of a primary developed cavity.

We have classified the mechanisms creating possibly erosive cavitation into five categories: the travelling cavity, shedding of an attached cavity, the upstream desinence, the upstream moving collapse, and creation of secondary cavities. On many occasions, secondary cavities arise as a sub process to the second and fourth classes of mechanisms above. They are in general, if they collapse close to a surface, erosive to some degree. The hydrodynamics dictating the generation of secondary cavitation is still not completely revealed, e.g. it seems clear that they foremost appear in shear layers with vortex roll-up, but to what extent the vortex formation is due mainly to viscous effects or Kelvin-Helmholtz instabilities is yet to be determined (although not crucial in any of the discussions in this paper).

In order to make design decisions related to the risks of erosion nuisance, it is necessary to capture the creation of the cavity, both the primary and the secondary, and trace its development towards collapse, but not necessarily record the actual collapse; this holds for both for experiments and numerical simulations. To be able to make quantitative predictions, also the collapse pulse amplitude needs to be recorded in both time and space. The important point is that it is not enough to study the collapse without it's history, partly since it will not be possible to make the correct design changes to avoid the problem and partly since the reliability of a simulation is questionable unless we know the correct mechanisms generating the collapse have been captured.

The implication of these conclusions is foremost that a good resolution, in both space and time, is necessary to be able to reveal enough of these mechanisms, in particular the creation of secondary cavities, in order to make a reliable erosion risk assessment. Concerning the importance of other considerations when choosing approach for the numerical simulation of cavitation, it is more difficult to make distinct statements at this stage. This concerns for example the inclusion of (at least local) compressibility effects, that improves simulation of the collapse pulse and acoustic interaction by capturing the rebound, or regarding a viscous or an Euler approach as both have proven to give promising results with respect to cavitation; however, one might argue that generally viscous simulations are preferred in engineering applications.

A final comment is that the small scales of cavitation that we have shown govern the dynamics, and thus need to be simulated, forms a challenge when aiming for erosion risk assessment through numerical simulation in applications. However, looking a few years ahead, we believe the grid sizes necessary to resolve these scales this will soon be manageable with the current trends in increasing model sizes. The seemingly true unsteadiness of the problem may become a greater problem. If the periodicity is not high enough in these process the theoretical foundation for simulating this with RANS is questionable, while truly unsteady approaches, like Euler or Large Eddy Simulations approaches will require very long simulations times. To be able to perform RANS simulations, we believe models for these small scale, unsteady processes, and their relation to the turbulence models, need to be developed; a seemingly very difficult task. The most promising approach for applications, thus seems to be a hybrid RANS/LES approach, where the steady non-cavitating flow may be simulated with RANS while the flow mechanisms governing cavitation can be resolved in time and space by LES.

ACKNOWLEDGEMENTS

The presented research has been financed through the European projects EROCAV, in the 5th EC framework programme, and VIRTUE, in the 6th EC framework programme. Computational resources were provided by Chalmers Centre for Computational Science and Engineering, C3SE.

REFERENCES

Bark, G., Berchiche N., and Grekula M. 2004, "Application of principles for observation and analysis of eroding cavitation, EROCAV observation handbook", Ed. 3.1, Chalmers University of Technology, Sweden, 2004.

Bark, G., Berchiche, N. and Grekula, M., 2004a, "A theoretical approach to an extended view of the development towards erosive cavitation", Proc. of the ITTC Cavitation Erosion Workshop, Val de Reuil, France, 2004-05-27—28.

Benjamin, T. B. and Ellis, A. T. 1966, “The collapse of cavitation bubbles and the pressure thereby produced against solid boudaries” Royal Soc. of London, Philosophical transactions, A, vol 260, pp. 221 – 240.

Bensow, R.E., Huuva, T., Bark G., Liefvendahl, M., 2008, ”Large Eddy Simulation of Cavitating Propeller Flows,” 27th Symp. on Naval Hydrodynamics, Seoul, Korea.

Brennen, C. E., 1995, “Cavitation and bubble dynamics”. Oxford University Press.

Ceccio, S.L. and Brennen, C.E., 1991, “Observations of the dynamics and acoustics of travelling bubble cavitation”, J. of Fluid Mech. Vol. 233, pp. 633 – 660.

Corcos, G. M. and Sherman, F. S. 1973, “Vorticity concentration and the dynamics of unstable free shear layers”, J. Fluid Mech. vol. 73, part 2, pp. 241-264.

Ellis, A. T. 1955, “Techniques for Pressure Pulse Measurements and High-Speed Photography in Ultrasonic Cavitation”, Symp. on Cavitation in Hydrodynamics, National Physical Laboratory, Teddington, U.K.

Foeth, E.-J., 2008, “The Structure of Three-Dimensional Sheet Cavitation,” PhD-thesis, Delft Univ. of Technology, Delft, The Netherlands.

Franc, J.P. and Michel, J.M., 1997, "Cavitation erosion research in France: the state of the art" Journal of Marine Science and Technology, Vol.2, pp.233-244.

Franc, J.-P. and Michel, J.-M., 2004, “Fundamentals of Cavitation”, Kluver Academic Publishers.

Grekula, M. and Bark, G., 2009, “Analysis of high-speed video data for assessment of the risk of cavitation erosion”. Proc. 1st Int. Conf. on Advanced Model Measurement Technology for EU Maritime Industry (AMT09), Nantes, 1-2 Sept. 2009, France.

Hallander, J. and Bark, G., 2002, ”Influence of acoustic interaction in noise generating cavitation“, 24th Symp. on Naval Hydrodynamics, Fukuoka, Japan.

Hickling, R. and Plesset, M. S. 1964, “Collapse and Rebound of a Spherical Bubble in Water”, Physics of Fluids, Vol. 7, No. 1, pp. 7 – 14.

Huuva, T., Cure, A., Bark, G., Nilsson, H., 2007, “Computations of unsteady cavitating flow on wing profiles using a volume fraction method and mass transfer models,” *Proceedings of the 2nd IAHR International Meeting,* Timisoara, Romania, October 24-26.

Huuva, T., 2008, “Large eddy simulation of cavitating and non-cavitating flow”, PhD thesis, Chalmers Univ. of Technology, Sweden.

Lecoffre, Y., 1999, “Cavitation – Bubble Trackers”, Balkema.

Mørch, K.A., 1982, “Energy considerations on the collapse of cavity clusters”, Applied Scientific Research 38: pp. 313 – 321, Martinus Nijhoff Publishers, The Hauge, Netherlands.

Mørch, K.-A., Bark, G., Grekula, M., Jønk, K.M., Nielsen P.L. and Stendys P., 2003, “The formation of cavity clusters/re-entrant jet contact”, 5th Int. Symp. on Cavitation, Osaka, Japan.

Patnaik, P. C., Sherman, F. S. and Corcos, G. M. 1973, “A numerical simulation of Kelvin-Helmholtz waves of finite amplitude”, J. Fluid Mech. vol. 73, part 2, pp. 215-240.

Schöön, J. 2000, “A method for the Study of Unsteady Cavitation – Observations on Collapsing Sheet Cavities,” PhD Thesis, Chalmers Univ. of Technology, Sweden.

Van der Meulen, J. H. J. and Van Renesse, R.L., 1988, “The collapse of bubbles in a flow near a boundary”, 17th Symp. on Naval Hydrodynamics, National Academy Press, Washington D.C., USA, 1989.

Wikström, N., Bark, G. and Fureby, C., 2003, “Large eddy simulation of submerged objects”, 8th Int. Conf. on Num. Ship Hydrodynamics, Busan, Korea.

APPENDIX

The experiments discussed in this paper were performed within the EU FP5 project EROCAV and the EU FP6 project VIRTUE. The simulations were all performed within VIRTUE.

The SSPA propeller P1477, was selected for the studies of the generation and synchronisation process for groups of vortex cavities. To avoid a wake from the shaft the propeller was operated in an inclined inflow, 8°, from the left as shown in Figure 20. To stabilise the cavitation and reduce light reflections the test object was painted with a roughened paint according to the SSPA standard.

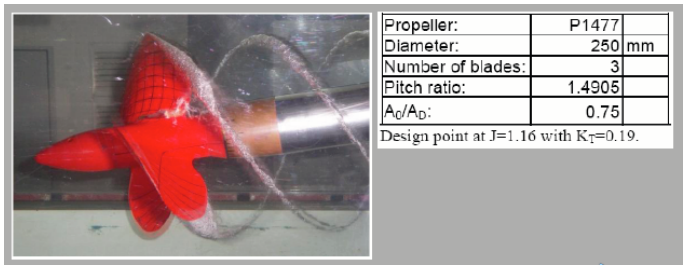

Figure 20 *Test set up for the propeller.*

As a supplement, also a 2-D foil with a profile selected from the propeller P1477 was made. This foil was operated at unsteady conditions generated by rotational oscillation around its mid-chord axis, a simplification in comparison to the gust generator earlier applied in this type of studies. This approximation of the similarity between the propeller and foil can be substantial in some conditions, Schoon (2000), but was supposed to be acceptable for the present aims. Another time saving selection made due to the reduced budget was that the foil was oriented vertically, a fact resulting in some visible influence of gravity. Often however the results were more disturbed by other 3-D cavitation behaviours than the gravity effect. To avoid a massive 3-D effect a transparent endplate was mounted at the free end of the foil. Detailed description of tests, protocols etc. are given in VIRTUE deliverable D4.4.2a. The cavitation in the present experiments was recorded by high-speed video with frame rates between 12 000 and 90 000 fps.

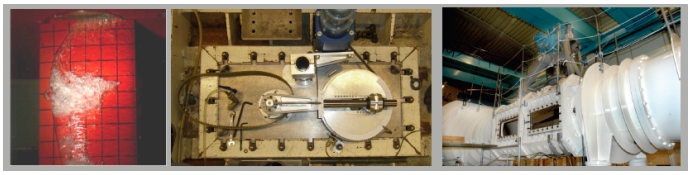

Figure 21 *The foil, oscillation set up and the high-speed test section.*